Published in final edited form as:
Microcirculation. 2011 May ; 18(4): 331–338. doi:10.1111/j.1549-8719.2011.00093.x.

Intravital Macrozoom Imaging and Automated Analysis of Endothelial Cell Calcium Signals Coincident with Arteriolar Dilation in Cx40^{BAC} GCaMP2 Transgenic Mice

POONEH BAGHER[1], **MICHAEL J. DAVIS**[1,2], and **STEVEN S. SEGAL**[1,2]

[1]Department of Medical Pharmacology and Physiology, University of Missouri, Columbia, MO 65212, USA

[2]Dalton Cardiovascular Research Center, Columbia, MO 65211, USA

Abstract

Objective—Calcium signaling is integral to endothelium-dependent vasodilation. Our goal was to develop methods enabling automated analyses for accurately and objectively determining the dynamic relationship between endothelial cell (EC) Ca^{2+} responses and arteriolar diameter *in vivo*.

Methods—User-friendly software (DiaFluor) written in LabView was applied to images acquired at 15 frames s^{-1} with a custom macrozoom intravital microscope to evaluate changes in EC Ca^{2+} concomitant with arteriolar diameter. Transgenic Cx40^{BAC}-GCaMP2 mice expressing a fluorescent Ca^{2+} indicator molecule in arteriolar ECs enabled resolution of EC Ca^{2+} signaling in response to acetylcholine (ACh) microiontophoresis (500 nA, 100-1000 ms pulse) from a micropipette (1 μm tip) positioned adjacent to an arteriole in the superfused cremaster muscle preparation.

Results—A 100-ms pulse of ACh (1M) had little effect on EC Ca^{2+} or arteriolar diameter. As pulse duration increased, vasodilation increased with fluorescence intensity ($P<0.01$). Based upon fluorescence responses (F/Fo), the effective diffusion distance of ACh along arterioles increased from ~100 μm (250 ms pulse) to ~200 μm (1000 ms pulse) with a peak velocity of ~150 μm s^{-1}.

Conclusions—The novel imaging and software presented here are the first to enable automated simultaneous evaluation of EC Ca^{2+} signaling and endothelium-dependent vasodilation *in vivo*.

Keywords

arteriole; imaging; microcirculation; DiaFluor software

INTRODUCTION

Intravital microscopy enables direct observation of the microcirculation in living systems. Whereas endothelium-dependent vasodilation is integral to the local control of tissue blood flow, the ability to study underlying Ca^{2+} events has required selective loading of endothelial cells (ECs) with indicator dyes (6, 8). In recent years, GCaMP2 has been developed as a bright and dynamic Ca^{2+} sensor based upon green fluorescent protein (GFP) (16). As connexin40 (Cx40) is expressed constitutively in arteriolar ECs of the mouse cremaster muscle (11), transgenic *Cx40^{BAC}-GCaMP2* mice were created using the Cx40 gene locus to localize GCaMP2 to arteriolar endothelium (15). Thus EC Ca^{2+} signaling

Correspondence: Steven S. Segal, Ph.D. Department of Medical Pharmacology and Physiology MA415 Medical Science Building University of Missouri - Columbia Columbia, MO 65212 tel: (573) 882-2553 fax: (573) 884-4276 segalss@health.missouri.edu.

events in arterioles can be studied *in vivo* without loading of Ca^{2+} indicator dyes (15) as GCaMP2 provides spatiotemporal resolution similar to that of such commonly used Ca^{2+} indicators as Fluo-4 (10). Moreover, the fluorescence signal originating in ECs provides an ideal reference for detecting luminal diameter, thereby overcoming difficulties inherent to automated microvessel edge detection that have otherwise restricted its use to isolated vessel preparations *in vitro* (4).

To study EC Ca^{2+} signaling *in vivo*, the original experiments performed on arterioles in GCaMP2 mice (15) relied upon manual frame-by-frame analyses of Ca^{2+} fluorescence and diameter. However such analyses are labor intensive and may introduce human error into the measurement, particularly during long recordings and with large data files. Therefore, a key goal of the present study was to develop and implement a user-friendly automated approach to acquiring and analyzing digital fluorescent imaging of the microcirculation. Given the ability of ACh to stimulate a rise in EC $[Ca^{2+}]_i$ (3), we developed a novel platform using macrozoom intravital imaging coupled with automated image analyses to simultaneously evaluate dynamic responses of Ca^{2+} fluorescence and arteriolar diameter. The delivery of vasoactive agents [e.g., the endothelium-dependent vasodilator acetylcholine (ACh)] to designated sites within the microcirculation is enabled by microiontophoresis (7). Whereas a vasoactive substance released from a micropipette exerts a direct action on the arteriolar wall, how the spatiotemporal aspects of this relationship are affected by stimulus intensity has remained ambiguous. Therefore, to illustrate the applicability of our system to intravital studies of the microcirculation, we investigated the nature of ACh diffusion from its site of release. Using microiontophoresis, we tested the hypothesis that with constant ejection current, the effective distance for ACh diffusion would increase with the duration of a stimulus pulse.

METHODS AND MATERIALS

Animal care and use

All procedures were approved by the Institutional Animal Care and Use Committee of the University of Missouri. Experiments were performed on Tg(RP24-25504-GCaAMP2)1Mik mice (generations N_4 to N_6 bred on C57BL/6J background) in the University of Missouri animal facility. Adult male $Cx40^{BAC}$-GCaMP2 mice (n=13; 6-8 months; 32±1g) were anesthetized with pentobarbital sodium [60 mg/kg, intraperitoneal injection] and the left cremaster muscle was prepared for intravital imaging (1). Exposed tissue was irrigated continuously with physiological saline solution (in mM: 131.9 NaCl, 4.7 KCl, 2 $CaCl_2$, 1.17 $MgSO_4$, 18 $NaHCO_3$) equilibrated with 5% CO_2 / 95% N_2 (pH 7.4, 34 °C). At the end of experiments the mouse was killed with an overdose of pentobarbital (intraperitoneal injection) followed by cervical dislocation.

Intravital imaging

Intravital imaging was performed on a custom fluorescence microscope based upon an Olympus MVX10 Stereo Zoom platform (Center Valley, PA). Using a mercury lamp, GCaMP2 was excited at 472/30 nm with emission at 520/35 nm. Images were acquired as tiff stacks through a MV PLAPO 2XC lens (numerical aperture = 0.50; Olympus) at 15 frames s^{-1} (fps) using an intensified digital camera [XR/Mega-10, Stanford Photonics Inc. (SPI); Palo Alto, CA] via Piper Control Software (SPI) on a personal computer. For the present experiments, total magnification was 167X with field of view (FOV) = 1100 μm X 885 μm.

Image analysis

Images were acquired at 15 frames/s for 10 s and tiff stacks were analyzed using custom software (DiaFluor) written in LabView (National Instruments, Austin, TX; *see* Supplemental Figure). The program has two major functional components: diameter tracking and line scan fluorescence detection; each was tested independently for precision and accuracy (*see Results*). While viewing on a digital monitor, the user creates a desired number of rectangular regions of interest (ROI) positioned normal to the vessel axis and adjusts threshold controls for detection of both edges of the arteriole. Fluorescence is recorded under resting conditions (Fo; mean of the first 5 frames) and during calcium responses (F; from baseline through recovery back to baseline). Fluorescence responses are detected along the ROI centerline spanning the vessel width and are presented as F/Fo in arbitrary units (Fig.1). Luminal diameter is tracked frame-by-frame as the outer edge of the fluorescent endothelium (Fig. 1B and 1D), using a slight modification of an iterative edge-detection algorithm described previously (4). Multiple ROIs provide fluorescence and diameter measurements at designated sites. Up to 10 ROIs have been used for the present experiments; however, the analysis slows with each additional ROI. The FOV calibration is adjustable to account for magnification changes and enables output of distances between ROI centerlines. Settings can be stored and recalled for subsequent analyses, enabling consistency in data acquisition sites across experimental conditions. User-defined distances between ROIs, which are output by the program following execution, further reduce variability in ROI placement.

For the present experiments, the first ROI was placed with its centerline aligned with the stimulus micropipette and defined as ‘Site 1’. Up to 10 consecutive sites were placed at 25-μm intervals upstream, enabling Ca^{2+} fluorescence and diameter responses to be evaluated at respective sites simultaneously (Fig. 1B). Fluorescence was recorded under resting baseline conditions (‘F_o’, mean of first 5 frames) and during Ca^{2+} responses (‘F’, baseline through recovery) with data presented as F/F_o (arbitrary units, AU). Peak F/F_o was taken for each ROI. DiaFluor output plots fluorescence and diameter frame-by-frame on the user interface with data saved in an Excel-compatible format. An image of the ROI sites on the final file of the tiff stack is also saved.

Micropipettes and Microiontophoresis

Borosilicate glass micropipettes (tip diameter, ~ 1 μm) were backfilled with ACh (1 M), secured in a micromanipulator and connected to a constant current source (model 260; World Precision Instruments; Sarasota, FL) via a silver wire. A second silver wire secured at the edge of the preparation served as the reference electrode. With retaining current set at 250 nA to prevent leakage, the tip of the ACh micropipette was positioned adjacent to an arteriole and the FOV was maintained throughout an experimental protocol.

Characterization of Ca^{2+} and Vasomotor Responses

Protocol 1: Stimulus duration—With ejection current held at 500 nA, ACh was delivered (random order) as a 100, 250, 500 or 1000 ms pulse with 3 min recovery between successive stimuli. Calcium fluorescence (F/F_o) and diameter responses were acquired adjacent to the micropipette tip and at 25-μm intervals along the arteriole upstream from the site stimulation. The velocity at which a fluorescence response spread was calculated as the time difference required for F/F_o at respective sites [($frame_{siteX}$-$frame_{site1}$) × 0.067 s] to reach threshold (defined as F > 2% above Fo) divided by the distance from Site 1. Diameter was recorded concurrently using fluorescence edge tracking. At the end of each experiment, sodium nitroprusside (SNP, 10^{-4} M) was added to the superfusion solution to obtain maximal diameter.

Protocol 2: Vasomotor tone—A submaximal stimulus (500 ms, 500 nA) was delivered under control conditions. The superfusate was then equilibrated with 21% O_2 (5% CO_2, balance N_2) for 8 min and the stimulus repeated. The superfusate was then re-equilibrated with 5% CO_2 / 95% N_2. Either norepinephrine (10^{-9}, 10^{-8} or 10^{-7} M) or SNP (10^{-4} M) was added to the superfusion solution for 3 min to achieve a stable baseline. The ACh stimulus was repeated under each condition with arteriolar vasomotor tone (%) calculated as: $[(D_{max} - D_{treatment}) / D_{max}] \times 100$, where D_{max} = diameter during SNP and $D_{treatment}$ = diameter during the particular treatment condition. Across treatments, fluorescence and diameter responses were sorted according to the prevailing level of vasomotor tone (~50%, 40%, 30%, 20% and D_{max}).

Data Analysis

Summary data represent independent observations from at least 5 mice and are presented as means ± S.E. Data were analyzed using analysis of variance, linear regression and Pearson correlation using Prism software (Version 5; GraphPad, La Jolla, CA). Differences were considered statistically significant with $P<0.05$.

RESULTS

Responses to ACh microiontophoresis

For a constant stimulus pulse (500 ms, 500 nA) $[Ca^{2+}]_i$ fluorescence increased adjacent to the micropipette (Fig. 1A) and decayed bidirectionally along the endothelium (*see* supplemental video). When 3 identical ACh stimuli were repeated at rest, peak F/F_o varied < 3% (n=7; intraclass correlation coefficient = 0.976, $P<0.001$), demonstrating that stimuli and responses were highly reproducible. As shown for analyses of sites located upstream from the stimulus, peak F/F_o decreased with distance (Fig. 1B &1C). Thus, even with a robust F/F_o response at Site 1, an increase in F/F_o was no longer detectable by Site 7 (distance = 150 μm). Coincident with the greatest F/F_o response, diameter responses at Site 1 were significantly greater ($P<0.05$) than at Sites 5 and 10 (Fig. 1D and E, n= 11; *see* supplemental video), where little or no change in F/F_o was observed. Increasing stimulus duration from 250 to 1000 ms produced a greater peak F/F_o response encompassing greater distance (Fig. 2A) and higher velocity (Fig. 2B). At Site 1, the magnitude of vasodilation increased with stimulus duration and then plateaued (Fig. 2C) with a significant correlation between peak F/F_o and the corresponding diameter change (Fig. 2D). With a constant stimulus pulse (500 ms, 500 nA), F/F_o responses to ACh were not different across levels of tone (Fig. 3A-3C) while the magnitude of vasodilation (i.e., diameter change) decreased predictably as vasomotor tone decreased (Fig. 3D).

Reference calibrations

Baseline total fluorescence did not differ significantly between rest and maximum diameters obtained with SNP (Figure 3A-B), indicating that changes in diameter independent of EC stimulation did not affect the GCaMP2 signal. The edge tracking function of our DiaFluor software was tested for accuracy by comparing the diameters (range, 1 to 47 μm) of fluorescent beads measured manually using video calipers with values obtained using DiaFluor. The relationship between diameter measurements made with video calipers vs. DiaFluor was linear ($y = 1.001x – 0.1508$; $r^2= 0.9996$; data not shown). As an independent reference for fluorescence measurements, we compared values from arterioles using SparkAn software [(12, 13) kindly provided by A. Bonev and M.T. Nelson, University of Vermont] with measurements using DiaFluor. After accounting for differences in how Fo is determined between respective programs (SparkAn uses the average of the lowest 10 mean intensity values), the relationship between F/Fo values obtained with DiaFluor and SparkAn was also linear ($y = 0.9974x – 0.0043$; $r^2= 0.9885$; data not shown). Thus we are confident

that DiaFluor accurately measures distance based upon fluorescent edge detection and that its evaluation of F/F_o is consistent with SparkAn software that has been validated for dynamic analyses of $[Ca^{2+}]_i$ fluorescence responses (12, 13) .

DISCUSSION

Local delivery of a stimulus from a micropipette using microiontophoresis has provided an effective tool for studying vasomotor responses underlying blood flow control in arteriolar networks (7, 14). Integral to vasodilation are endothelium-mediated signalling events governed by a rise in $[Ca^{2+}]_i$. The intravital macrozoom imaging and analysis techniques presented here have enabled concomitant automated evaluation of the dynamics between Ca^{2+} signaling in ECs and arteriolar diameter *in vivo* for the first time. Using transgenic mice expressing GCaMP2, a GFP-based Ca^{2+} sensor in arteriolar endothelium, we show that, when delivered as a brief pulse (500 nA, ≤ 1 s) from a micropipette (1 μm tip) positioned adjacent to the arteriolar wall, the direct actions of ACh are constrained to a radius of ~200 μm. The GCaMP2 protein was genetically engineered to incorporate a Ca^{2+}/calmodulin domain such that fluorescence increases in response to a rise in $[Ca^{2+}]_i$ (17). Using a bacterial artificial chromosome, the expression of GCaMP was directed to microvascular ECs in accord with the constitutive expression of Cx40 in arteriolar endothelium (11, 15). A complementary genetic approach to studying smooth muscle cell Ca^{2+} regulation of vasomotor responses in vivo was recently demonstrated in studies in which a FRET-based Ca^{2+}/calmodulin-activated myosin light chain kinase biosensor was genetically encoded in vascular smooth muscle cells of transgenic mice (18). The use of genetically encoded Ca^{2+} indicators promises to provide important new insight into complex signaling events in vivo (9).

Automated real-time tracking of vessel diameter in isolated vessels has been based upon resolving a clear distinction between differences in the optical intensity of ‘light’ and ‘dark’ boundaries associated with the vessel lumen and the internal and external edges of the vessel wall (4). Difficulties encountered within intravital preparations include multiple ‘edges’ in the tissue and red blood cell obstruction of the vessel lumen. These limitations are particularly acute in the cremaster muscle where striated muscle fibres present contrasting edges in multiple directions, confounding discrete tracking. This limitation was overcome here by tracking the boundary of intrinsic EC fluorescence from GCaMP2 to measure the luminal diameter of arterioles. Key requirements are sharp focus of the arteriolar wall and sufficient contrast between the arteriolar lumen and surrounding tissue. Highlights of this system include user-defined ROIs for signal analysis and concomitant tracking of Ca^{2+} fluorescence responses (F/F_o) with luminal diameters. The ability to track multiple regions of interest along an arteriole is facilitated by the thinness of the cremaster muscle complemented by the outstanding field of view, working distance and optical section thickness afforded by macrozoom imaging.

To measure EC Ca^{2+} fluorescence responses, the user defines ROIs positioned normal to the vessel axis. Responses are detected along ROI centerlines spanning the vessel width and are presented as F/Fo in arbitrary units. While the intensity of F_o can vary between experiments, normalizing F to the prevailing F_o enables comparisons across preparations as well as between sites of interest in arteriolar networks. Despite the inability to ascertain actual $[Ca^{2+}]_i$, the dynamic range of the fluorescent signal we obtained from $Cx40^{BAC}$-GCaMP2 mice enabled resolution of key spatiotemporal features of ACh delivered from micropipettes. The effective distance and apparent velocity that fluorescence increased along arterioles increased with stimulus duration in a highly reproducible manner (Fig. 2A and B). Regression analysis at Site 1 indicates a proportionality between the increase in EC $[Ca^{2+}]_i$ fluorescence and the increase in arteriolar diameter, such that a 50% increase in F/F_o

corresponded to a diameter change of ~10 μm (Fig. 2D). These findings substantiate the interpretation that signaling events initiated by a rise in EC $[Ca^{2+}]_i$ (e.g., activation of $K_{Ca}3.1$ and $K_{Ca}2.3$ channels and endothelial nitric oxide synthase) lead to smooth muscle cell relaxation (3, 5).

A key concern when evaluating $[Ca^{2+}]_i$ responses is whether a change in arteriolar diameter alone alters the fluorescence signal. To determine whether such an effect occurred in the present experiments, we measured total fluorescence across the vessel (under the line scan) and found that it was not significantly altered during maximal vasodilation with SNP in the superfusate (Fig. 3A and 3B), an NO donor that promotes vasodilation independent of the endothelium. Previous work utilizing the GCaMP2 mice demonstrated that local delivery of SNP from a micropipette produced arteriolar dilation without a rise in Ca^{2+} (15). Collectively, these data suggest that changes in arteriolar diameter alone (i.e., independent of activating Ca^{2+} signaling in ECs) do not influence GCaMP2 fluorescence *in vivo*.

The increase in fluorescence decayed with distance from Site 1 such that $[Ca^{2+}]_i$ responses were no longer distinguishable from F_o beyond ~150 μm. As fluorescence responses were bidirectional along arterioles (Fig. 1A), we estimate that under the experimental conditions used here the effective diffusion distance for ACh to act directly on the arteriolar wall is < 200 μm. Finding that F/F_o responses along arterioles were highly reproducible and independent of the level of vasomotor tone (Fig. 3C) is consistent with this interpretation and illustrates that the ability of muscarinic receptor activation to trigger a rise in EC $[Ca^{2+}]_i$ is independent of the contractile status of surrounding smooth muscle cells. The relationships illustrated in Figure 2 indicate that increasing the release of ACh (e.g., with greater ejection current, stimuli of longer duration, and with pressure ejection of bulk fluid) are likely to encompass greater distances for direct effects along the vessel wall. In our previous experiments, ACh was delivered using greater ejection current (1 μA) and F/F_o increased for distances of up to 400 μm (15). Consistent with these earlier findings, the magnitude of vasodilation along arterioles was greatest in regions where $[Ca^{2+}]_i$ increased (Fig. 1D and E). Moreover, observing that vasodilation extended beyond the region of $[Ca^{2+}]_i$ responses (Fig.1E) is consistent with the initiation and conduction of hyperpolarization from cell to cell through gap junctions along the arteriolar wall, promoting smooth muscle relaxation through electromechanical coupling at distances well beyond changes in EC $[Ca^{2+}]_i$ (2, 5, 15).

Summary and Conclusion

We present novel methods for acquiring and analyzing EC Ca^{2+} dynamics and arteriolar vasomotor responses based upon intravital macrozoom imaging of $Cx40^{BAC}$-GCaMP2 mice. In arterioles controlling blood flow to the cremaster muscle, we illustrate that internal diameter and F/F_o (reflecting EC $[Ca^{2+}]_i$) increase with the duration of an ACh stimulus delivered locally from a micropipette using microiontophoresis. The increase in F/F_o decays along arterioles with an effective diffusion distance for ACh of < 200 μm and is not influenced by changes in vasomotor tone. The methodology presented here can now be used to address an array of questions focused on endothelium-dependent Ca^{2+} signaling in the intact microcirculation during blood flow control.

Supplementary Material

Refer to Web version on PubMed Central for supplementary material.

Acknowledgments

Grant support: This work was supported by the National Institutes of Health grants R37-HL041026 (SSS), F32-HL097463 & T32-AR048523 (PB), and P01-HL095486 (MJD) from the United States Public Health Service. DiaFluor is freely available for academic use; please contact MJD at davismj@missouri.edu for download instructions.

Abbreviations used

ACh	acetylcholine
Cx40	connexin40
EC	endothelial cell
FOV	field of view
F	fluorescence response
Fo	baseline fluorescence
fps	frames per second
GFP	green fluorescent protein
ROI	region of interest
SNP	sodium nitroprusside
tiff	tagged image file format

REFERENCES

1. Bagher P, Duan D, Segal SS. Evidence for impaired neurovascular transmission in a murine model of Duchenne Muscular Dystrophy. J Appl Physiol. 2011; 110:601–609. [PubMed: 21109597]
2. Bagher P, Segal SS. Regulation of blood flow in the microcirculation: Role of conducted vasodilation. Acta Physiol. 2011 doi: 10.1111/j.1748-1716.2010.02244.x.
3. Busse R, Fichtner H, Luckhoff A, Kohlhardt M. Hyperpolarization and increased free calcium in acetylcholine-stimulated endothelial cells. Am J Physiol. 1988; 255:H965–969. [PubMed: 3177686]
4. Davis MJ. An improved, computer-based method to automatically track internal and external diameter of isolated microvessels. Microcirculation. 2005; 12:361–372. [PubMed: 16020082]
5. Domeier TL, Segal SS. Electromechanical and pharmacomechanical signalling pathways for conducted vasodilatation along endothelium of hamster feed arteries. J Physiol. 2007; 579:175–186. [PubMed: 17138602]
6. Dora KA, Xia J, Duling BR. Endothelial cell signaling during conducted vasomotor responses. Am J Physiol. 2003; 285:H119–126.
7. Duling BR, Berne RM, Born GVR. Microiontophoretic application of vasoactive agents to the microcirculation of the hamster cheek pouch. Microvasc Res. 1968; 1:158–173.
8. Duza T, Sarelius IH. Localized transient increases in endothelial cell Ca2+ in arterioles in situ: implications for coordination of vascular function. Am J Physiol. 2004; 286:H2322–2331.
9. Kotlikoff MI. Genetically encoded Ca2+ indicators: using genetics and molecular design to understand complex physiology. J Physiol. 2007; 578:55–67. [PubMed: 17038427]
10. Ledoux J, Taylor MS, Bonev AD, Hannah RM, Solodushko V, Shui B, Tallini Y, Kotlikoff MI, Nelson MT. Functional architecture of inositol 1,4,5-trisphosphate signaling in restricted spaces of myoendothelial projections. Proc Natl Acad Sci U S A. 2008; 105:9627–9632. [PubMed: 18621682]
11. Looft-Wilson RC, Payne GW, Segal SS. Connexin expression and conducted vasodilation along arteriolar endothelium in mouse skeletal muscle. J Appl Physiol. 2004; 97:1152–1158. [PubMed: 15169746]

12. Perez GJ, Bonev AD, Patlak JB, Nelson MT. Functional coupling of ryanodine receptors to KCa channels in smooth muscle cells from rat cerebral arteries. J Gen Physiol. 1999; 113:229–238. [PubMed: 9925821]

13. Petkov GV, Nelson MT. Differential regulation of Ca2+-activated K+ channels by beta-adrenoceptors in guinea pig urinary bladder smooth muscle. Am J Physiol. 2005; 288:C1255–1263.

14. Segal SS, Duling BR. Flow control among microvessels coordinated by intercellular conduction. Science. 1986; 234:868–870. [PubMed: 3775368]

15. Tallini YN, Brekke JF, Shui B, Doran R, Hwang SM, Nakai J, Salama G, Segal SS, Kotlikoff MI. Propagated endothelial Ca2+ waves and arteriolar dilation in vivo: measurements in Cx40BAC GCaMP2 transgenic mice. Circ Res. 2007; 101:1300–1309. [PubMed: 17932328]

16. Tallini YN, Shui B, Greene KS, Deng KY, Doran R, Fisher PJ, Zipfel W, Kotlikoff MI. BAC transgenic mice express enhanced green fluorescent protein in central and peripheral cholinergic neurons. Physiol Genomics. 2006; 27:391–397. [PubMed: 16940431]

17. Wang Q, Shui B, Kotlikoff MI, Sondermann H. Structural basis for calcium sensing by GCaMP2. Structure. 2008; 16:1817–1827. [PubMed: 19081058]

18. Zhang J, Chen L, Raina H, Blaustein MP, Wier WG. In vivo assessment of artery smooth muscle [Ca2+]i and MLCK activation in FRET-based biosensor mice. Am J Physiol. 2010; 299:H946–956.

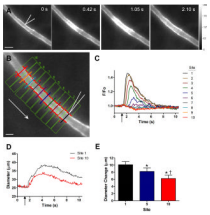

Figure 1.

Automated simultaneous tracking of arteriolar diameter and Ca^{2+}fluorescence. **A**) Four sequential images of arteriolar Ca^{2+} fluorescence. Bidirectional rise in fluorescence indicates changes in $[Ca^{2+}]_i$ along the endothelium in response to ACh (500 ms, 500 nA) at times indicated (first panel: micropipette tip outlined in white; scale bar = 50 μm and applies to each panel). **B**) Arteriolar segment upstream from stimulus micropipette with 10 adjacent ROIs (green boxes). Within each ROI is a central scan line, perpendicular to the direction of flow, for measuring integrated fluorescence from the vessel wall. Respective scan lines are positioned ~25 μm apart, colors correspond with tracings in C. Red dots indicate luminal edges tracked for diameter. Arrow indicates direction of blood flow; micropipette tip outlined in white. Scale bar = 25 μm. **C**) Representative traces of fluorescence responses (F/F_o) from each scan line in B. The fluorescence response decayed with distance and was no longer distinguished from baseline at Site 7 (~150 μm). **D**) Representative traces of lumen diameter at Site 1 (where maximum fluorescence occurred) and Site 10 (no fluorescence change). Vertical arrow indicates ACh stimulus delivery. **E**) Summary data (n= 11) for diameter measurements in the presence (Site 1 and Site 5) and absence (Site 10) of a fluorescence response. * Vasodilation (Diameter Change) at Sites 5 and 10 significantly different from Site 1 ($p < 0.05$). † Vasodilation at Site 10 significantly different from Site 5 ($p < 0.05$).

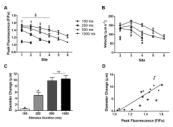

Figure 2.

Calcium fluorescence, ACh diffusion velocity and vasodilation. Experimental design and recording sites are as in Fig. 1B. **A**) With constant ejection current (500 nA), peak F/Fo and diffusion distance increased with ACh stimulus pulse duration (n=6). A 100 ms ACh pulse had negligible effect. In response to a 250 ms ACh pulse, the increase in F/F_o was not different from baseline beyond 75 μm (Site 4). § Peak F/Fo decreased with distance (Sites 1-4; $P<0.01$). † Significant difference between peak F/F_o in response to 250 ms vs. other stimulus durations ($P<0.05$). ‡ Significant difference between peak F/F_o responses among all stimulus durations ($P<0.05$). **B**) The velocity at which F/F_o spread along arterioles tended to decay with distance. Higher velocities occurred with longer stimulus durations. # Significant difference between 250 ms and 1000 ms ($P<0.05$). **C**) At the site of stimulation (Site 1), vasodilation increased with ACh pulse duration up to 500 ms and then plateaued. * Significantly different vs. other stimulus durations ($P<0.05$). ns, not significantly different. **D**) With spontaneous vasomotor tone, vasodilation at Site 1 increased with peak fluorescence across stimulus intensities ($r^2= 0.69$; $P<0.01$).

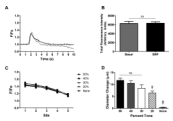

Figure 3.

Fluorescence responses across levels of vasomotor tone. For these experiments, the ACh stimulus was constant (500 ms, 500 nA). **A**) Recorded at Site 1, representative traces of Ca^{2+} fluorescence (F/F_o) in response to ACh with spontaneous vasomotor tone and during maximal dilation with SNP (black). **B**) Summary data (n=5) for total fluorescence intensity across the width of an arteriole during spontaneous vasomotor tone (resting diameters, 20-30 μm) vs. during maximal vasodilation with SNP (diameters, 40-50 μm; n= 5). **C**) Peak Ca^{2+} fluorescence at Sites 1-5 (see Figure 1B) under varying levels of vasomotor tone. Peak F/F_o was not different across levels (up to 50%) of vasomotor tone (n=5 each). **D**) Vasodilation (Diameter Change, recorded at Site 1) was greatest at higher levels of vasomotor tone. ns, not significantly different. † Significantly different vs. 50% tone ($P<0.05$). ‡ Significantly different vs. other levels of tone ($P<0.05$).